

Duality Between Organic Photoconductor Thickness and Print Engine Parameters

Jang Yi[▲]

BEL 324, MRC Institute, University of Idaho, Moscow, Idaho 83844-1024

E-mail: jang@mrc.uidaho.edu

Richard B. Wells

BEL 316, MRC Institute, University of Idaho, Moscow, Idaho 83844-1024

E-mail: rwells@uidaho.edu

Abstract. *The correlation between organic photoconductor (OPC) thickness and several printer parameters and OPC aging are theoretically analyzed. We found that linewidth changes from varying the charge transport layer (CTL) thickness are analogous to those from adjusting several printer parameters. Thus, the same linewidths and print quality can be achieved by appropriately adjusting those parameters, provided that lateral motion of photogenerated charge carriers during their transit from the charge generation layer to the CTL surface is negligibly small. In particular, it is found that the laser power is required to increase exponentially with respect to an increase in CTL thickness in order to maintain the same linewidths, and the power sensitivity is inversely proportional to the quantum efficiency. In addition, it is found that, under certain conditions, varying the CTL thickness is analogous to adjusting several print engine parameters. © 2006 Society for Imaging Science and Technology. [DOI: 10.2352/J.ImagingSci.Technol.(2006)50:2(193)]*

INTRODUCTION

The thickness of an organic photoconductor (OPC) is an important design parameter in electrophotography. One of the reasons a very thin OPC is desirable is because lateral motion of photogenerated charge carriers and the transit time from the charge generation layer (CGL) to the charge transport layer (CTL) surface are reduced,^{1–4} which corresponds to a high print speed. However, it is difficult to manufacture thin OPCs and they have a larger relative variation in charge (at constant voltage) resulting in a larger variance in print results. OPC aging is another factor in image degradation. In this paper, we theoretically analyze the effects of CTL thickness and OPC aging, and present the observed correlation between the CTL thickness and several printer parameters in monocomponent development systems with relatively less transparent CTLs. Nominal print engine parameters used in our calculations, unless noted otherwise, are given in Table I.

LATENT IMAGE FORMATION WITH VARYING OPC THICKNESS

Light intensity at a distance z beneath the OPC surface decays exponentially⁵

$$I = I_{\text{surf}} e^{-kz}, \quad (1)$$

where I_{surf} is the intensity at the surface ($z=0$) and k is the absorption coefficient (see Fig. 1). For a typical single layer OPC of thickness d , Chen reported that⁶

$$k = \frac{4.6}{d}. \quad (2)$$

For $d=20 \mu\text{m}$, $k=0.23 \mu\text{m}^{-1}$, which is comparable to an earlier finding for a polymer at a radiation wavelength of 600 nm reported by Schaffert.⁷ In a dual layer photoconductor (PC), it is the amount of light absorbed in the CGL that determines the quantity of photogenerated charge carriers. Thus, the thicker the CTL, the less light is absorbed in the CGL, resulting in a smaller charge distribution. When $k=0.23 \mu\text{m}^{-1}$, only about 1% of the intensity at the surface reaches the CGL. A typical CTL would have to be much less opaque. Extrapolating from Schaffert's data, the absorption coefficient at 700 nm is about $0.07 \mu\text{m}^{-1}$, where about 25% of the surface intensity reaches the CGL. The absorption coefficient can vary significantly depending on OPC materials. In particular, the absorption coefficient of a single layer OPC tends to be much greater than that of a dual layer OPC since photons are to penetrate the CTL and reach the CGL in dual layer OPCs whereas they are to be absorbed and convert their energy to the creation of charge carriers before they reach the ground substrate in single layer OPCs. Thus, the absorption coefficient of a typical dual layer OPC may be much smaller than $0.07 \mu\text{m}^{-1}$.

The intensity at the CTL/CGL boundary can be utilized to obtain the corresponding exposure energy G at the boundary

$$G(d) = G_{\text{surf}} e^{-kd}, \quad (3)$$

where G_{surf} is the surface exposure.^{1,8,9} The surface potential and exposure are related via photoinduced discharge characteristics (PIDC)

[▲]IS&T Member

Received Sep. 30, 2003; accepted for publication Jun. 16, 2005.

1062-3701/2006/50(2)/193/9/\$20.00.

Table I. Printer parameters.

Parameter	Description	Value
P	Laser power	0.1 mW
v	Scan velocity	1000 m/s
t_r	Laser rise time	2 ns
t_f	Laser fall time	2 ns
S_x	x spot size ($1/e^2$)	60 μm
S_y	y spot size ($1/e^2$)	60 μm
V_{sat}	Saturation voltage	-100 V
V_{dark}	Dark voltage	-800 V
G_a	PC sensitivity	0.2 $\mu\text{J}/\text{cm}^2$
V_{bias}	Developer bias	-500 V
ρ	Toner volume charge density	-20 $\mu\text{C}/\text{cm}^3$
ϵ_{PC}	PC dielectric constant	3
ϵ_t	Toner dielectric constant	3
λ	Toner layer thickness	5 μm
g	Developer gap	5 μm
d_0	CTL thickness	20 μm

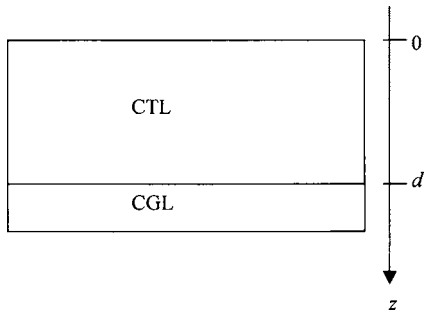
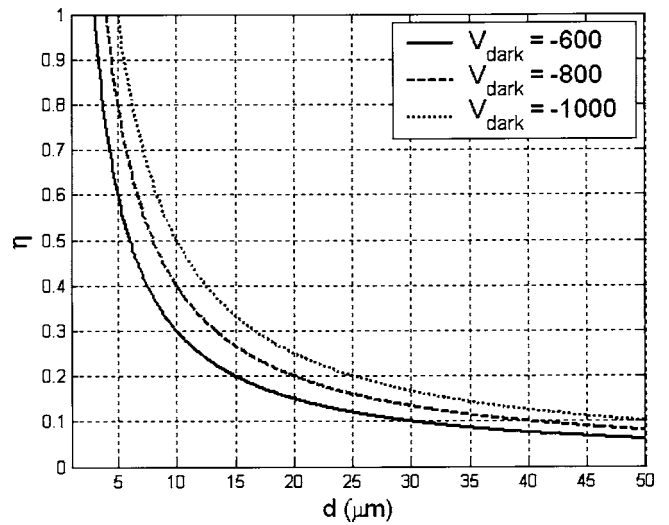


Figure 1. Layered photoconductor.

$$V = V_{\text{sat}} + (V_{\text{dark}} - V_{\text{sat}}) \left[\exp\left(-\frac{G_{\text{surf}}}{G_a}\right) \right], \quad (4)$$

where V_{sat} is the saturation voltage (large exposure voltage), V_{dark} is the dark voltage (initial voltage before exposure), and G_a is the PC sensitivity. Note that this experimental characterization is designed for solid area latent image formation. For arbitrary patterns, assuming complete lateral independence, we obtain the surface charge distribution from Eq. (4) as


 Figure 2. Quantum efficiency for $V_{\text{dark}} = -600, -800,$ and -1000 V.

$$\sigma_{\text{surf}} = \sigma_{\text{sat}} + (\sigma_{\text{dark}} - \sigma_{\text{sat}}) \left[\exp\left(-\frac{G_{\text{surf}}}{G_a}\right) \right], \quad (5)$$

where

$$\sigma_{\text{sat}} = \frac{\epsilon_0 \epsilon_{\text{PC}} V_{\text{sat}}}{d} (\text{C}/\text{m}^2) \quad \text{and} \quad \sigma_{\text{dark}} = \frac{\epsilon_0 \epsilon_{\text{PC}} V_{\text{dark}}}{d} (\text{C}/\text{m}^2). \quad (6)$$

ϵ_0 is the permittivity of free space and ϵ_{PC} is the PC dielectric constant. The quantity of the arrived carriers σ_{arrived} is the difference between Eq. (5) and σ_{dark} ,

$$\sigma_{\text{arrived}} = (\sigma_{\text{dark}} - \sigma_{\text{sat}}) \left[\exp\left(-\frac{G_{\text{surf}}}{G_a}\right) - 1 \right]. \quad (7)$$

Typically, PIDC measurements are taken for a fixed CTL thickness d_0 . Thus Eq. (7) can be written as

$$\begin{aligned} \sigma_{\text{arrived}} &= \frac{\eta(d)}{\eta(d_0)} (\sigma_{\text{dark}} - \sigma_{\text{sat}}) \left\{ \exp\left[-\frac{G_{\text{surf}}}{G(d_0)} \frac{G(d)}{G_a}\right] - 1 \right\} \\ &= \frac{\eta(d)}{\eta(d_0)} (\sigma_{\text{dark}} - \sigma_{\text{sat}}) \left[\exp\left(-\frac{G_{\text{eff}}}{G_a}\right) - 1 \right], \end{aligned} \quad (8)$$

where

$$G_{\text{eff}} = e^{-k(d-d_0)} G_{\text{surf}} \quad (9)$$

and $\eta(d)$ is the quantum efficiency defined as the number of incident photons into the CGL per charge carrier generated and conducted through the CTL. η is in general field and intensity dependent. Shaffert found that the intensity dependence is very small and we approximate his field dependent η data with a straight line⁷

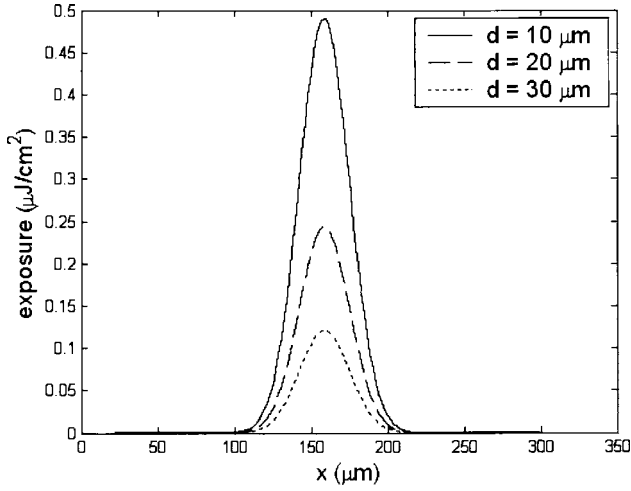
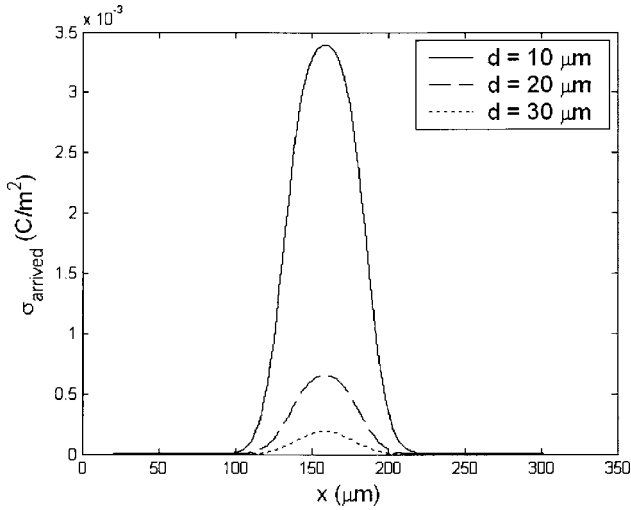


Figure 3. Exposure dependence on CTL thickness.


 Figure 4. σ_{arrived} for $d = 10, 20,$ and $30 \mu\text{m}$.

$$\eta(d) \approx 0.005 \times 10^6 E_z(d) = 0.005 \times 10^6 \frac{|V_{\text{dark}}|}{d} (\text{V/m}), \quad (10)$$

where E_z is the initial normal field in the CTL. This approximated field dependent quantum efficiency reaches its maximum value 1.0 when $d = d_{\text{min}} = 0.005 \times 10^6 |V_{\text{dark}}|$ ($d_{\text{min}} = 4 \mu\text{m}$ for $V_{\text{dark}} = -800 \text{ V}$), indicating lossless generation and transport of charge carriers for $d \leq d_{\text{min}}$. Figure 2 shows the approximated quantum efficiency for $V_{\text{dark}} = -600, -800,$ and -1000 V .

The effect of the CTL thickness in Eq. (8) is twofold. First, the number of photons entering the CTL/CGL boundary varies with d . Second, the carrier generation and conduction efficiency based on these photons also vary with d due to the initial field variation in the film from the constant potential difference and varying film thickness. Calculated

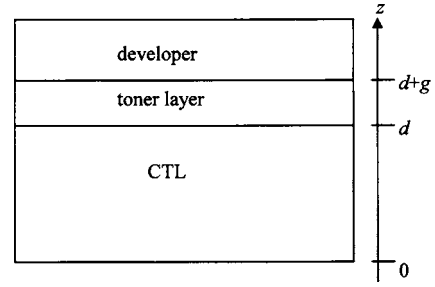
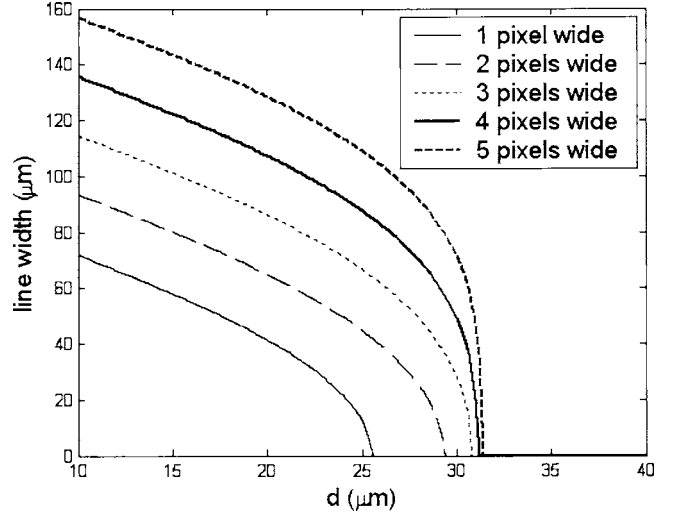


Figure 5. Development region geometry.


 Figure 6. Calculated linewidths of 1, 2, 3, 4, and 5 pixel wide lines ($k = 0.07 \mu\text{m}^{-1}$).

values of G_{eff} and σ_{arrived} for a single-pixel-wide vertical line for $d = 10, 20,$ and $30 \mu\text{m}$ are shown in Figs. 3 and 4, respectively. These figures show drastic changes in exposure and charge solely due to PC thickness variation. In some dual layer OPCs, latent images can vary relatively little even when d increases by $8 \mu\text{m}$.¹⁰ Thus, k appears to be very material dependent and an experimentally verified value for k of a given OPC is required for a more quantitative assessment on latent image variation arising from different OPC thicknesses.

DEVELOPMENT CALCULATION

The development region geometry is shown in Fig. 5. The normal electric field E_z in the developer gap can be calculated in the spatial frequency domain^{11,12}

$$\bar{E}_z(k_x, k_y, z) = \frac{\bar{\sigma}_{\text{surf}}(k_x, k_y)}{\epsilon_0 \epsilon_{\text{PC}}} \left\{ \begin{aligned} & \cosh[k_u(z-d)]u(z-d) \\ & - \frac{\cosh(k_u z) \sinh[k_u g]}{\sinh[k_u(g+d)]} \end{aligned} \right\} - k_u V_{\text{bias}} \delta(k_x, k_y) \frac{\cosh(k_u z)}{\sinh[k_u(g+d)]}$$

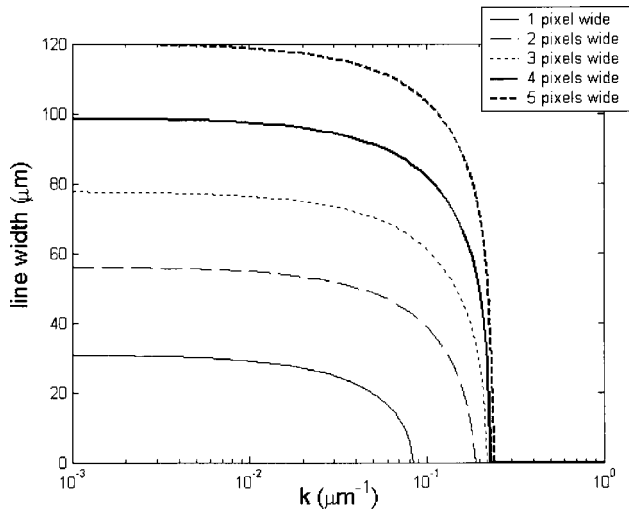


Figure 7. Calculated linewidths of 1, 2, 3, 4, and 5 pixel wide lines ($d=25 \mu\text{m}$).

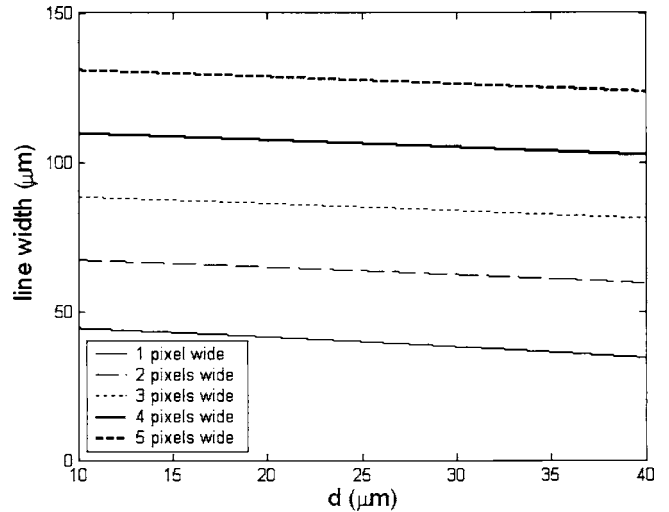


Figure 9. Calculated linewidths of 1, 2, 3, 4, and 5 pixel wide lines with $\eta=1.0$ ($k=0.01 \mu\text{m}^{-1}$).

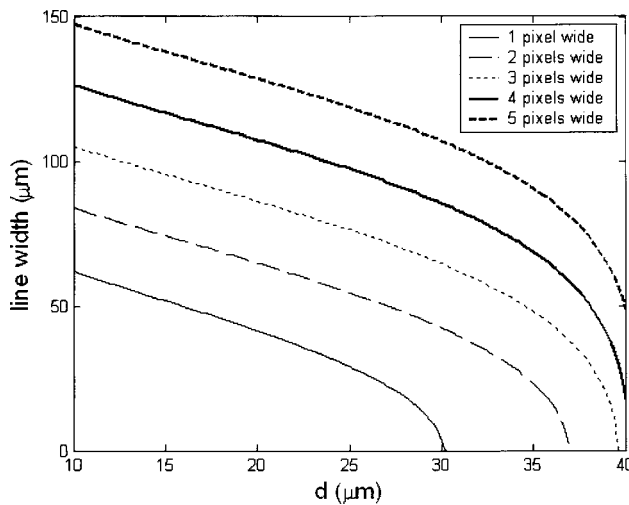


Figure 8. Calculated linewidths of 1, 2, 3, 4, and 5 pixel wide lines with the field dependent quantum efficiency ($k=0.01 \mu\text{m}^{-1}$).

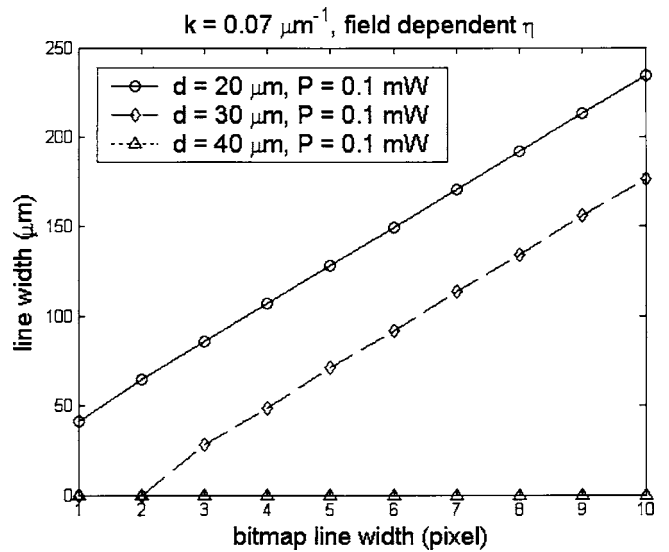


Figure 10. Developed linewidths (calculated) of ten vertical lines with $d=20, 30,$ and $40 \mu\text{m}$. The quantum efficiency is field dependent and the laser power is set to 0.1 mW .

$$\begin{aligned}
 & + \frac{\rho \cdot \delta(k_x, k_y)}{\epsilon_0 \epsilon_t k_u} (\sinh[k_u[z-d]]u(z-d) \\
 & - \sinh\{k_u[z-(d+\lambda)]\}u[z-(d+\lambda)]) \\
 & - \frac{\rho \cdot \delta(k_x, k_y) \{ \cosh(k_u g) - \cosh[k_u(g-\lambda)] \}}{\epsilon_0 \epsilon_t k_u} \\
 & \times \frac{\cosh(k_u z)}{\sinh[k_u(g+d)]}, \tag{11}
 \end{aligned}$$

where g is the developer gap, λ is the toner layer thickness, V_{bias} is the developer bias voltage, ρ is the toner volume charge density, ϵ_t is the toner dielectric constant, $u(\cdot)$ is the unit step function, $\delta(\cdot)$ is the Dirac delta function, $\bar{\sigma}_{\text{surf}}$ is the two-dimensional (2D) Fourier transform of $\sigma_{\text{dark}} + \sigma_{\text{arrived}}$, $k_u = \sqrt{k_x^2 + k_y^2}$, and k_x and k_y are the spatial fre-

quency variables in the x and y directions, respectively. We assume that development begins to take place when $E_z > 0$. Figure 6 shows the developed widths of 1, 2, 3, 4, and 5 pixel wide vertical lines using $k=0.07 \mu\text{m}^{-1}$. The developed widths decrease very rapidly with increasing CTL thickness d . This is qualitatively consistent with a previously reported finding that a few micron increase in PC thickness results in a noticeable development change.¹³ Figure 6 shows that when $d > 32 \mu\text{m}$, most of the photons are absorbed in the CTL and all of the five lines do not develop at all. Figure 7 shows the developed widths of the five vertical lines with $d = 25 \mu\text{m}$ as functions of absorption coefficient k . The linewidths vary little when $k < 0.01 \mu\text{m}^{-1}$, which suggests that using $k=0.01 \mu\text{m}^{-1}$ may result in little linewidth variation even for a large CTL thickness. However, even when k

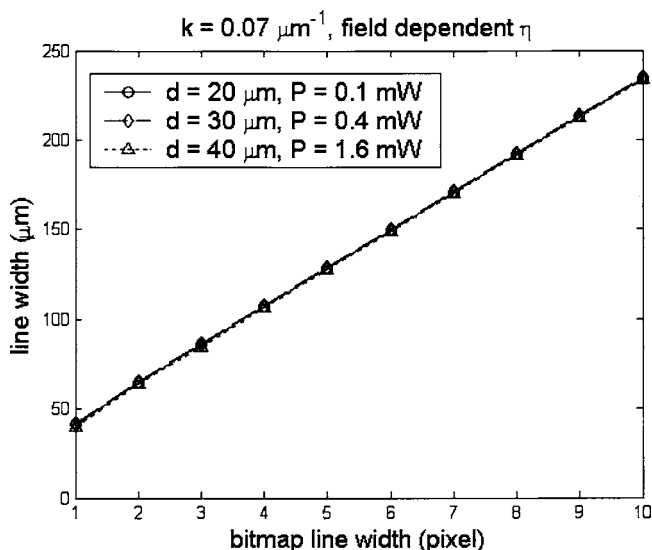


Figure 11. Developed linewidths (calculated) of ten vertical lines with $d=20, 30,$ and $40 \mu\text{m}$. The quantum efficiency is field dependent and the laser power is set to 0.1, 0.4, and 1.6 mW for $d=20, 30,$ and $40 \mu\text{m}$, respectively.

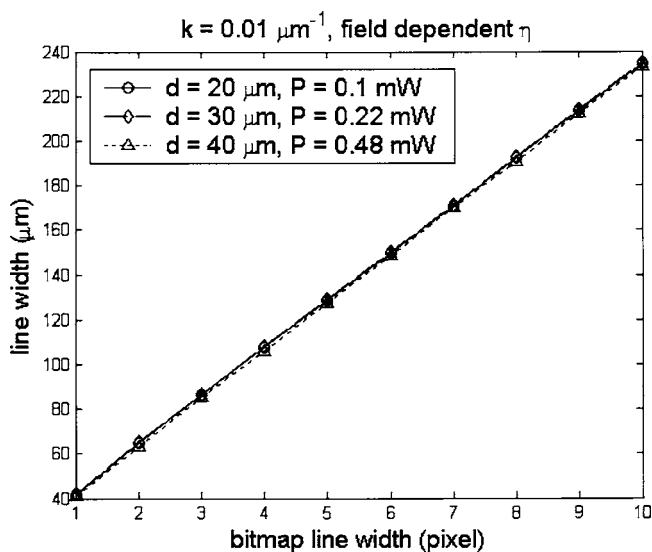


Figure 12. Developed linewidths (calculated) of ten vertical lines with $d=20, 30,$ and $40 \mu\text{m}$. The quantum efficiency is field dependent and the laser power is set to 0.1, 0.22, and 0.48 mW for $d=20, 30,$ and $40 \mu\text{m}$, respectively.

$=0.01 \mu\text{m}^{-1}$, as shown in Fig. 8, the first three lines do not develop before the CTL thickness falls below $40 \mu\text{m}$. This is mainly due to the field dependent quantum efficiency. When $\eta=1.0$ independent of the CTL thickness, the linewidth in fact changes little with d , as illustrated in Fig. 9. The quantum efficiency is likely to be intimately correlated with the absorption coefficient. However, due to a lack of quantitative information on their relationship, we will use the field dependent quantum efficiency and treat k and η as independent variables in this paper.

The CTL thickness is desired to be very thin to counteract photon absorption in the CTL and meet various de-

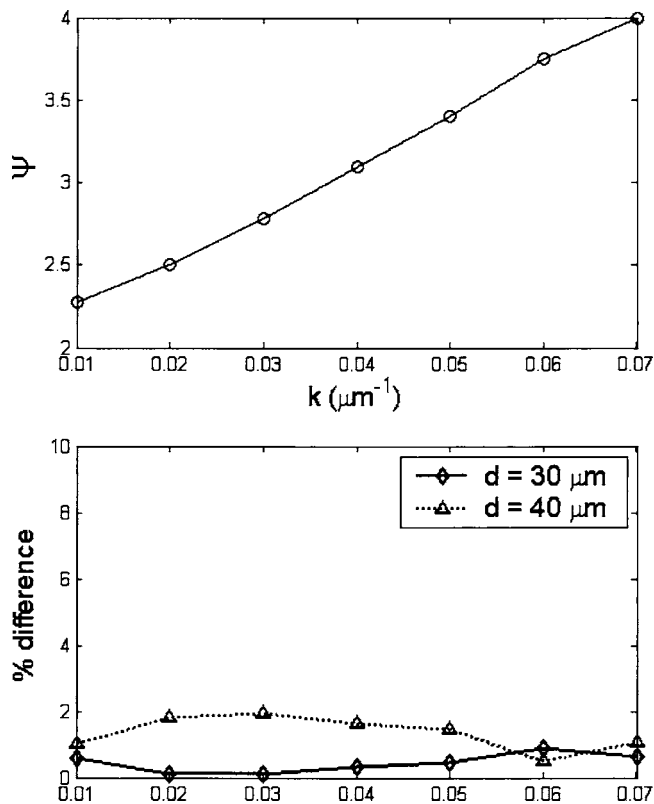


Figure 13. ψ and % difference (calculated).

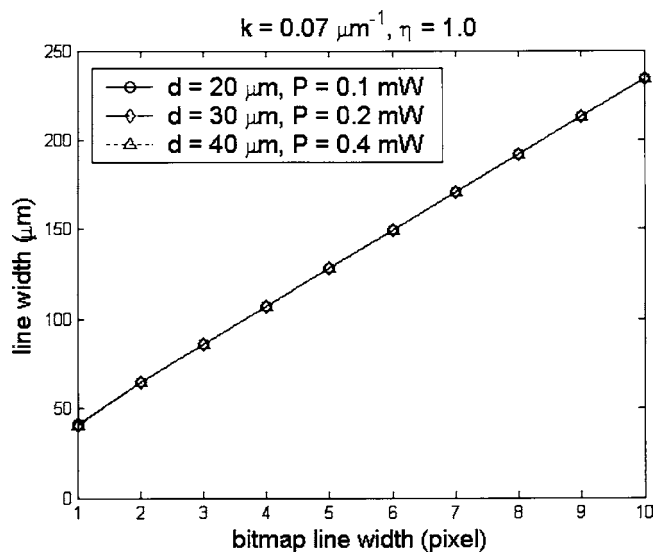


Figure 14. Developed linewidths (calculated) of ten vertical lines with $d=20, 30,$ and $40 \mu\text{m}$. The quantum efficiency is set to 1.0 and the laser power is set to 0.1, 0.2, and 0.4 mW for $d=20, 30,$ and $40 \mu\text{m}$, respectively.

velopment criteria. However, d cannot be made arbitrarily thin because PC aging and wear (as much as a few micron decrease in CTL thickness) need to be accounted for and such constraints are bound to increase manufacturing costs. In the next two sections, we show that a relatively thick OPC

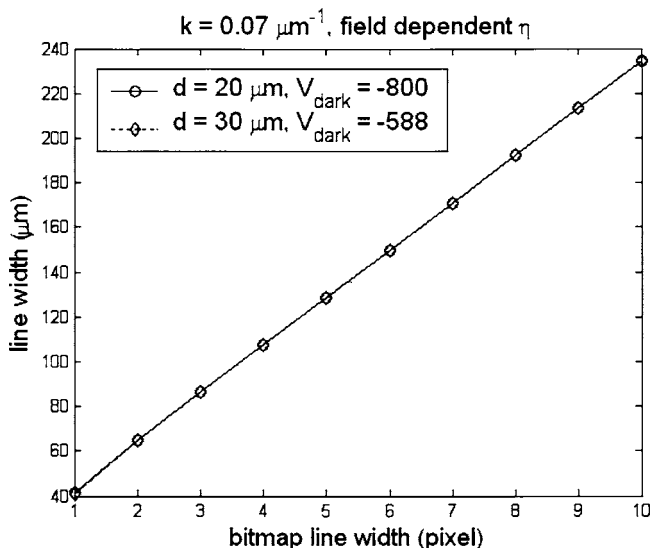


Figure 15. Developed linewidths (calculated) of ten vertical lines with $d=20$ and $30 \mu\text{m}$. The dark voltage is changed from -800 to -588 V .

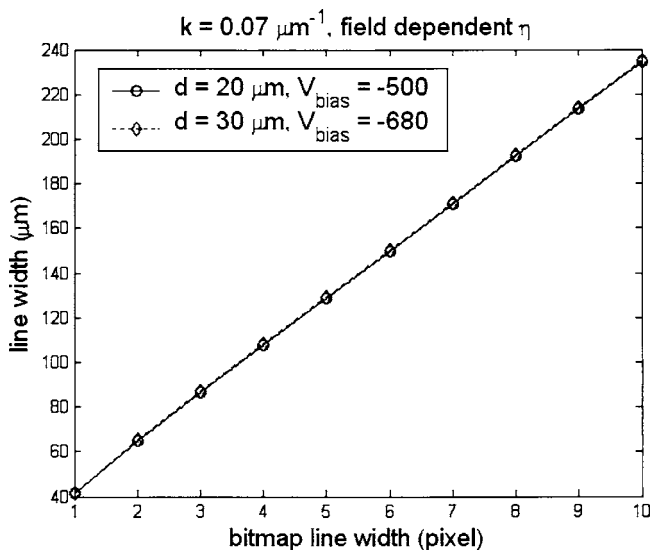


Figure 16. Developed linewidths (calculated) of ten vertical lines with $d=20$ and $30 \mu\text{m}$. The bias voltage is changed from -500 to -680 V .

can be used to reproduce the same linewidths as those with a thinner OPC by appropriately adjusting several printer parameters.

DUALITY OF CTL THICKNESS AND LASER POWER

Figure 10 shows the developed widths of ten vertical lines of widths one through ten pixels for $d=20, 30,$ and $40 \mu\text{m}$. At the bias voltage setting given in Table I, the $40 \mu\text{m}$ CTL does not allow any of the lines to develop. Since both k and η tend to reduce the effective number of photons, photon losses arising from a large CTL thickness can be compensated for by increasing the laser power P , provided that lateral motion of photogenerated charge carriers during their transit from the CGL to the CTL surface is negligibly small.³

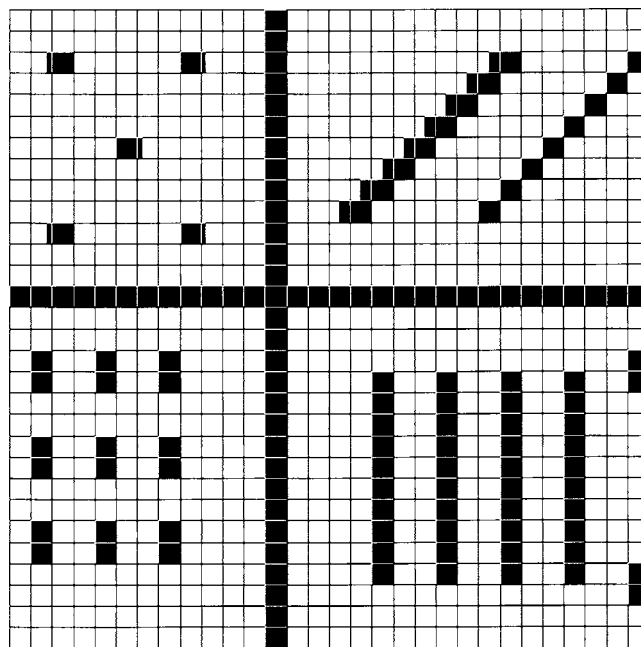


Figure 17. Bitmap.

It has been observed that increasing the laser power increases image sizes.¹⁴ Figure 11 shows the developed widths of the ten lines with the power for $d=30$ and $40 \mu\text{m}$ increased from 0.1 to 0.4 and 1.6 mW , respectively. The linewidths for all three CTL thicknesses are in good agreement. This suggests that

$$P = P_0 \times 2^{\psi(d-d_0)/d_0} = P_0 \times e^{0.6931\psi(d-d_0)/d_0}, \quad (12)$$

where P_0 is the laser power for $d=d_0$ and ψ specifies the power sensitivity to CTL thickness. ψ is dependent on k and η and it was set to 4.0 in Fig. 11. Figure 12 shows the developed widths of the ten lines with $k=0.01 \mu\text{m}^{-1}$. In this case, the power is increased to 0.22 and 0.48 mW for $d=30$ and $40 \mu\text{m}$, respectively, which resulted in $\psi=2.275$. Figure 13 shows ψ for various k values and the percent difference between the linewidths from $d=20 \mu\text{m}$ and the linewidths from $d=30$ and $40 \mu\text{m}$. For all k values, the linewidths from the three CTL thicknesses are in good agreement (less than 2% difference), which shows the duality between these two parameters. That is, the same linewidths can be maintained even when the CTL thickness increases by exponentially increasing the laser power according to Eq. (12).

The power sensitivity ψ is found to be inversely proportional to the quantum efficiency. This is qualitatively intuitive since the more efficiently the photons generate and conduct charge carriers through the CTL, the less increase in power would have to be required. Figure 14 shows the developed widths of the ten lines for the extreme case where the quantum efficiency is set to 1.0 for the three CTL thicknesses ($k=0.07 \mu\text{m}^{-1}$). The laser power was set to 0.2 and 0.4 mW for $d=30$ and $40 \mu\text{m}$, respectively. The developed linewidths for all three CTL thicknesses are in good agree-

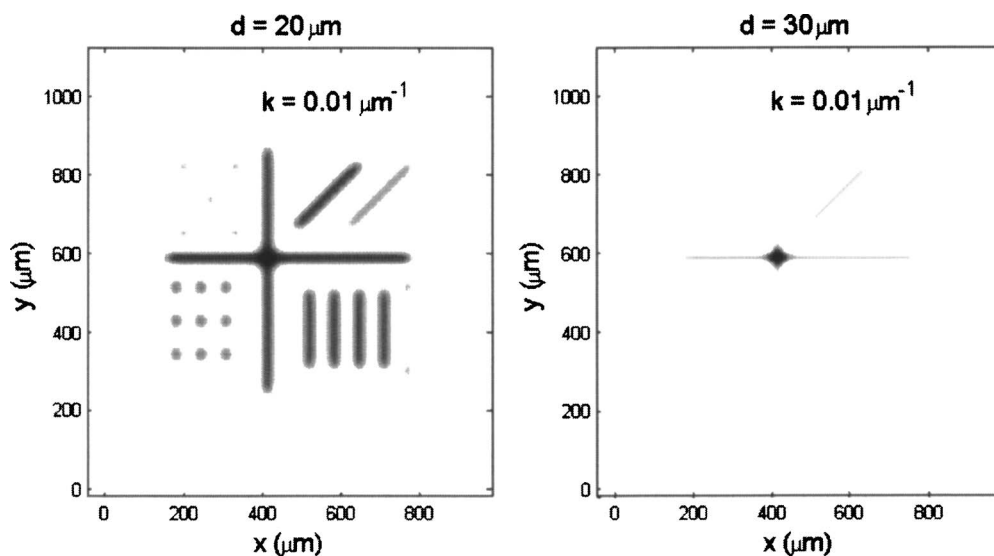


Figure 18. Calculated electric field of the pattern in Fig. 17. Gray scale represents field strength (the darker the development field, the stronger it gets).

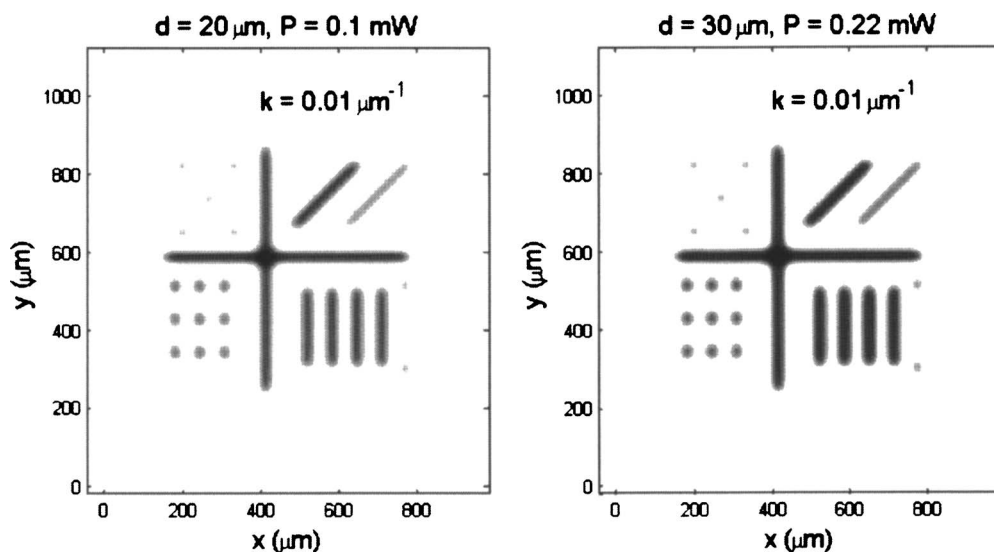


Figure 19. Calculated electric field of the pattern in Fig. 17. The laser power is increased from 0.1 to 0.22 mW.

ment. The resulting power sensitivity $\psi=2.0$ is lower than the value obtained from $k=0.01 \mu\text{m}^{-1}$. A more quantitative experimental characterization of k and η may be required to better understand the physical correlation between these parameters and laser power.

CORRELATION BETWEEN CTL THICKNESS AND OTHER PRINTER PARAMETERS

Varying the CTL thickness is also found to be analogous to adjusting other printer parameters such as the dark voltage and bias voltage. Figure 15 shows the developed widths of the ten lines with dark voltages -800 and -588 V for $d=20$ and $30 \mu\text{m}$, respectively, which coincide with each other. This shows that linewidth variation from changing the CTL thickness can be compensated for by adjusting the dark

voltage. Similarly, the developed linewidth changes from using different bias voltages for the two CTL thicknesses are shown in Fig. 16. The lines for both cases are in good agreement. Thus, it appears that the same linewidths from two different CTL thicknesses can be maintained by appropriately adjusting the dark or bias voltages.

2D EXAMPLES

Consider the bitmap shown in Fig. 17. The electric field at the CTL surface for $k=0.01 \mu\text{m}^{-1}$ and $d=20$ and $30 \mu\text{m}$ is shown in Fig. 18. Most of the feature for $d=30 \mu\text{m}$ does not develop due to the increase in CTL thickness. Increasing the power from 0.1 to 0.22 mW brings the field very close to that for $d=20 \mu\text{m}$, as illustrated in Fig. 19. Similarly, Figs. 20 and 21 show the field after the dark and bias voltages are

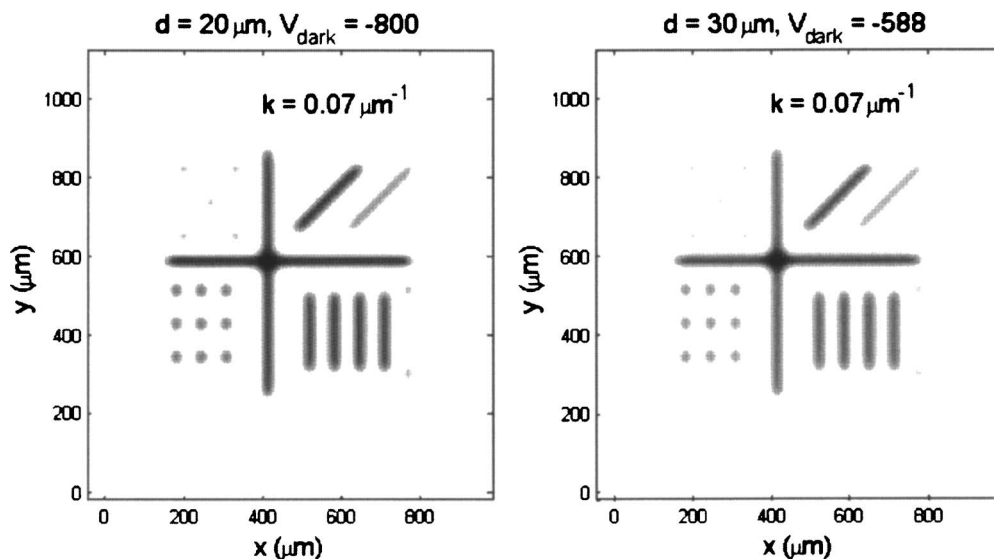


Figure 20. Calculated electric field of the pattern in Fig. 17. The dark voltage is changed from -800 to -588 V.

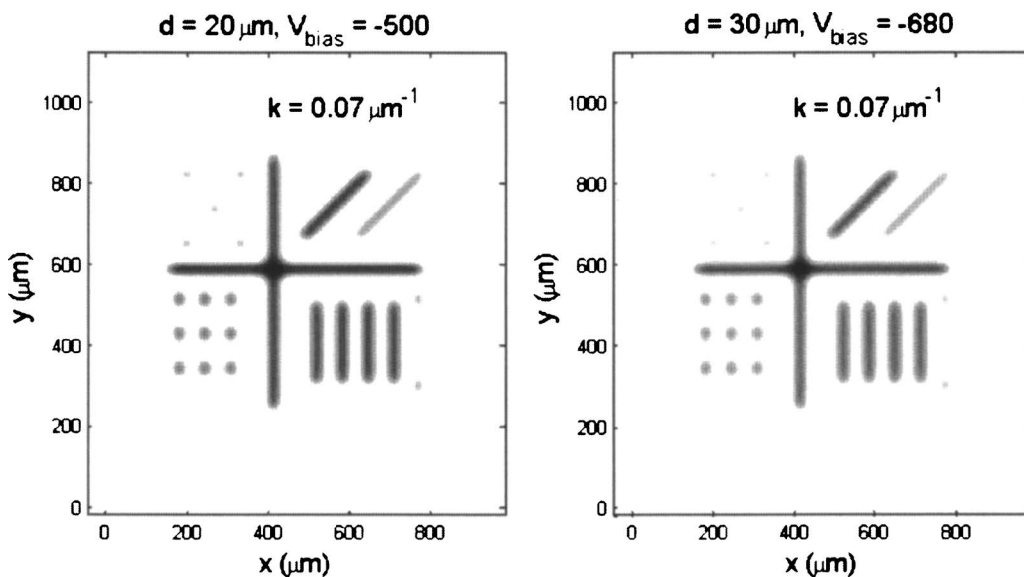


Figure 21. Calculated electric field of the pattern in Fig. 17. The bias voltage is changed from -500 to -680 V.

appropriately adjusted, respectively, as discussed in the previous section. After the adjustments, the images for $d = 30 \mu\text{m}$ very closely resemble the field plot for $d = 20 \mu\text{m}$, which verifies our conjecture that varying the CTL thickness is analogous to adjusting the laser power, dark voltage, or bias voltage.

LINewidth VARIATION FROM OPC AGING

It is found that increasing the CTL thickness does not necessarily compromise the OPCs robustness. A print engine with a thick CTL can be resilient to OPC aging as well. Figure 22 shows the linewidth changes after the CTL thickness is decreased by $2 \mu\text{m}$. The linewidth variation resulting from reducing d from 30 down to $28 \mu\text{m}$ after adjusting the

three parameters (power, dark, and bias voltages) are comparable to those from reducing d from 20 down to $18 \mu\text{m}$. Figures 23 and 24 show the linewidth changes from 10% power and G_a reduction, respectively. Once again, the linewidth variation resulting from adjusting the three parameters are comparable to those from $d = 20 \mu\text{m}$. Assuming physical wear (reduction in d) is the main mechanism for OPC aging, these figures indicate that OPC aging may be one of the predominant factors for image degradation.

CONCLUSIONS

We theoretically showed that after increasing the CTL thickness, the same linewidths can be achieved by appropriately adjusting the laser power, dark voltage, or bias voltage. In

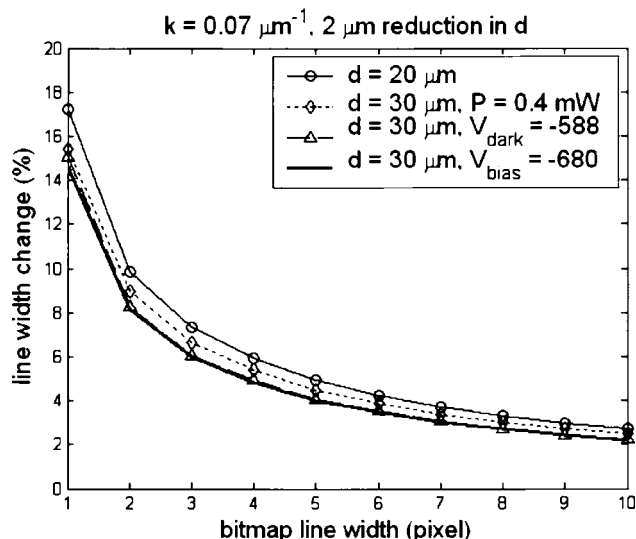


Figure 22. Calculated linewidth variation from 2 μm reduction in d .

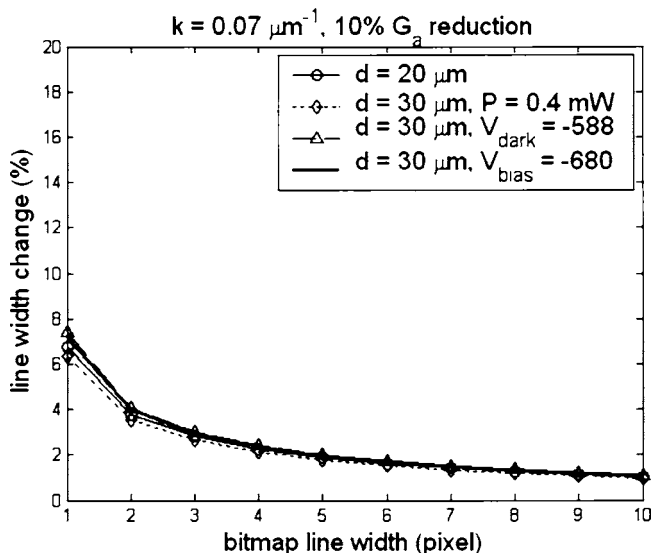


Figure 24. Calculated linewidth variation from 10% G_a reduction.

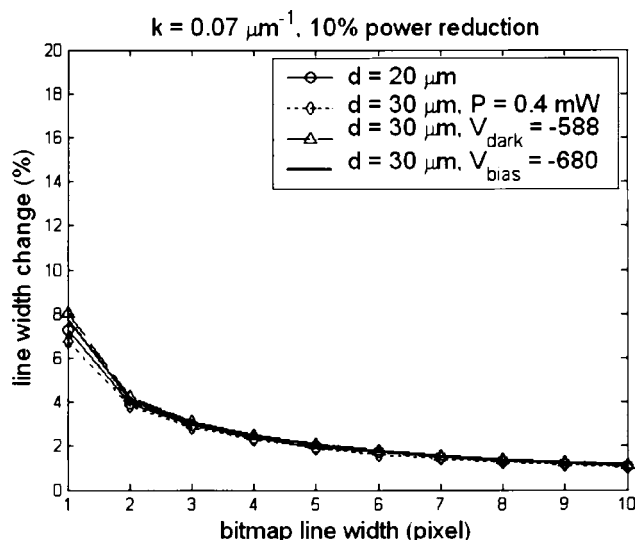


Figure 23. Calculated linewidth variation from 10% power reduction.

particular, it was found that the laser power is required to increase exponentially with respect to the increase in CTL thickness. Our findings lead us to believe that high resolution image reproduction can be achieved even with a fairly thick OPC, provided that lateral motion of photogenerated charge carriers during their transit from the CGL to the CTL surface is negligibly small. The CTL thickness cannot be made arbitrarily large because it would require more time to form latent images on the surface due to the longer transit time for the carriers, which will result in a longer process time and limit the print speed. However, we found that, within a given range of CTL thickness, adjusting the three

printer parameters (power, dark voltage, and bias voltage) can have almost the same end effect as changing the CTL thickness. This duality between the CTL thickness and the printer parameters allows one to more effectively optimize the parameters without compromising the print quality.

REFERENCES

- ¹E. M. Williams, *The Physics and Technology of Xerographic Processes* (Krieger, Malaba, FL, 1993).
- ²I. Chen, "Optimization of photoconductors for digital electrophotography", *J. Imaging Sci.* **34**, 15–20 (1990).
- ³J. Yi and R. B. Wells, "PC surface charge density from a vertically Gaussian, laterally exposure-based volume charge distribution in the CGL", *Proc. IS&T's NIP19* (IS&T, Springfield, VA, 2003) pp. 91–96.
- ⁴Y. Wanatabe, H. Kawamoto, H. Shoji, H. Suzuki, and Y. Kishi, "A numerical study of high resolution image formation by laser beam exposure", *J. Imaging Sci. Technol.* **45**, 579 (2001).
- ⁵A. Nussbaum and R. A. Phillips, *Contemporary Optics for Scientists and Engineers* (Prentice-Hall, Englewood Cliffs, NJ, 1976).
- ⁶I. Chen, "Nature of latent images formed on single layer organic photoreceptors", *Proc. IS&T's NIP18* (IS&T, Springfield, VA, 2002) pp. 404–408.
- ⁷R. M. Schaffert, "A new high-sensitivity organic photoconductor for electrophotography", *IBM J. Res. Dev.* **15**, 75–89 (1971).
- ⁸J. Yi, "A xerographic simulation model", M.S. thesis, University of Idaho, Moscow ID, May 1999.
- ⁹J. Yi and Richard B. Wells, "Power modulated exposure calculation", *J. Imaging Sci. Technol.* **48**, 287 (2004).
- ¹⁰K. Aizawa, M. Takeshima, and H. Kawakami, "A study of 1-dot latent image potential", *Proc. IS&T's NIP17* (IS&T, Springfield, VA, 2001) pp. 572–575.
- ¹¹C. C. Kao, "Electric field, transfer, and spread functions in xerographic image studies", *J. Appl. Phys.* **44**, 1543 (1973).
- ¹²J. Yi, R. B. Wells, and T. Camis, "Electric field calculation based on PIDC in monocomponent development systems", *Proc. IS&T's NIP18* (IS&T, Springfield, VA, 2002) pp. 23–27.
- ¹³T. Iwamatsu, T. Toyoshima, N. Azuma, Y. Mutou, and Y. Nakajima, "A study of high resolution latent image forming and development", *Proc. IS&T's NIP15* (IS&T, Springfield, VA, 1999) pp. 732–735.
- ¹⁴Y. Furuya, "Single dot development and threshold laser power on laser beam printer", *Proc. IS&T's NIP14* (IS&T, Springfield, VA, 1998) pp. 436–439.